NON-LINEARITIES IN TENSILE CREEP OF CONCRETE AT EARLY AGE

Anders Boe Hauggaard and Lars Damkilde
Department of Structural Engineering and Materials
Technical University of Denmark

ABSTRACT

A material model for creep is proposed which takes into consideration some of the couplings in early age concrete. The model is in incremental form and reflect the hydration process where new layers of cement gel are formed in a stress free state. In the present context attention is on non-linear creep at high stress levels. The parameters in the model develop in time as a result of hydration. The creep model has been used to analyse the tensile experiments at different stress levels carried out in the HETEK project. The tests were made on dogbone shaped specimen and the test procedure is described. Furthermore, compressive creep at high stress levels are fitted.
Key words: early age concrete, tensile creep, high stress levels, incremental creep model, couplings

1 INTRODUCTION

Concrete at early age is characterised by chemical reactions between cement particles and moisture which give the strength and stiffness development and also develop heat. The important factors are the temperature development, the moisture development and the development of the material properties.
The factors are coupled, e.g. the distribution of moisture has influence on the heat diffusion properties and moisture has to be present for the hydration to proceed. Experiments indicate that the hydration process also is coupled to the loading, /1/.
In order to predict the thermal stresses, which may cause cracking in the early age after casting, numerical models for the creep behavior are needed. The tensile stress level may be high and non-linearities in creep may occur. Creep is of importance because the relaxation of stresses influences the risk of cracking. The knowledge about non-linearities in tensile creep is scarce and complications arise due to the development of the properties as a result of hydration.
The relation between creep of concrete in tension and in compression is uncertain. Particularly, it is unclear whether non-linearities occur at high tensile stress levels similarly to the compressive non-linearities. In /2,3/ different parameters are used to model creep in tension and compression. In the present part of the HETEK project, control of early age cracking, tensile creep experiments were carried out in order to investigate non-linearities in creep at early age, see e.g. /4/. The work was a cooperation between The Danish Concrete Institute, The Danish Technological Institute and Technical Universities in Lyngby and Aalborg, Denmark. The HETEK project was funded by the Danish Road Directorate. The load levels were 40%, 60% and 80% of the tensile strength and the age at loading was 24 hours. Due to the development of the strength the load was increased every 24 hours.

A numerical model has been established which takes into consideration the increase in creep observed at high stress levels. The model is in incremental form and the concept of incremental material models is discussed. The development of the properties are taken into consideration explicitly and thermodynamic restrictions are fulfilled. The influence of the current stress level on the creep behavior is included with a correction factor on the material properties. Hereby the material properties in the model are reduced with increasing stress level.

2 CREEP EXPERIMENTS AT HIGH TENSILE STRESSES

Axi-symmetric dogbone specimens have been developed. The moulds are shown in Fig. 1 together with a specimen. Steel cups are glued to the specimen and loading is applied through

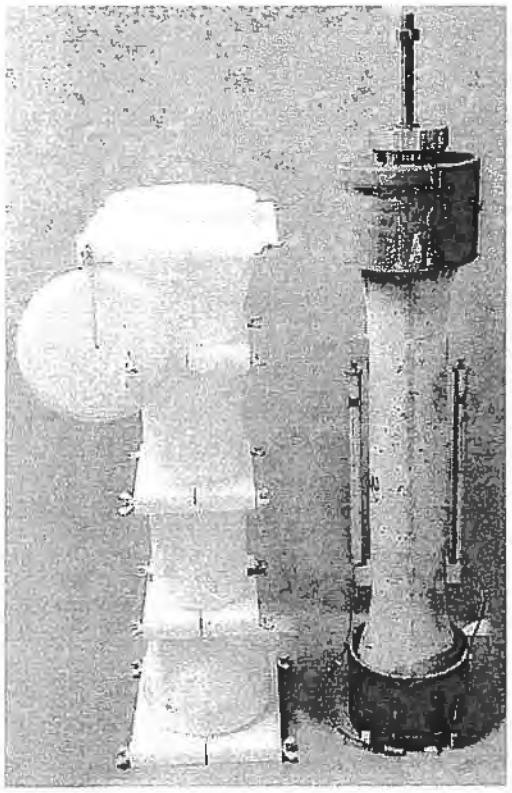

Figure 1: Tensile creep specimen. Teflon mould and specimen glued into steel cups.

heads with low friction hinges. Hereby bending in the specimen is reduced. The moulds are made of teflon and they are flexible with a cylindrical shaped center and two conical shaped ends. The total length of the specimen is 960 mm and the length of the cylindrical section is 480 mm. The diameter of the ends is 190 mm and the diameter of the cylindrical section is 130 mm. The conical zone between the end and the cylindrical section has a radius of curvature of 125 mm. These dimensions make it possible to test concrete with a maximum nominal aggregate size, d_{max}, of 32 mm according to a Danish standard, see e.g. /5/. The steel cup has an inner diameter of 200 mm resulting in a thickness of the glue layer of 5 mm as prescribed by the manufacturer.
After casting the moulds were placed horizontally to avoid settlement cracking and minimise differences in strength development due to gravity, see e.g. /6/. The specimens were cured in the moulds during the first 24 honrs. Then the steel cups are glued to the specimens and they are sealed and fastened in the testing machine. Sealing is carried out with welded alu-coated

plastic foil bags and heavy tape. For testing whether the sealing was sufficient an analysis was carried out, see e.g. /4/. Three different types of sealing were used for a 100 mm $\times$ 200 mm cylinder. The weight loss in time was recorded. The sealing types were

- 3 layers of thin plastic foil of thickness 12 μm
- 6 layers of thin plastic foil of thickness 12 μm
- the alu-coated plastic bags used in the present context

The plastic foil showed a weight loss measured as percentage of the mix-water of 23% for the 3 layers and 16% for the 6 layers within the 40 days testing period. In the case of the alu-coated plastic bags less than 0.1% weight loss took place. The water loss should be minimised as it may affect the shrinkage. The LVDT's used for the strain measurements have been attached in Fig. 1 and the sealing is removed for clarity. The connection mounts between the concrete and the heads of the LVDT's are fastened to steel pins with a diameter of 6 mm. Until demoulding the steel pins are fastened to the moulds. Since the steel pins cover a diameter in the specimen average deformations are measured. The measurement length is 400 mm. Stiff steel blocks are mounted to the steel pins and the LVDT is placed in between as seen in Fig. 1. A high stiffness of the connection was found to be important since an accuracy of the order of 5 μ-strain is needed for the tensile creep and shrinkage measurements. Rotation of the pins when fastening the steel blocks is avoided by two blade nuts screwed against each other on the pins in the middle of the specimen. In the experiments the strains measured on the loaded specimen have to be compensated for thermal and shrinkage strains. These strains are measured on an unloaded dummy which is kept together with the loaded specimen to obtain the same temperature and drying history.
The temperature is measured in the center and near the surface of each specimen at the cross-section where the pins are located. Temperature measurements are started immediately after casting to determine whether gradients occur. The environmental temperature is kept constant at about 24°C. The measurements in the center and the surface region showed only little difference. During the first 24 hours the temperature increases from the environmental temperature of 24°C to 28.5°C. After demoulding the temperature is within the range 25.5°C to 23.5°C. The age at loading is 24 hours and three tensile load levels, 0.4, 0.6 and 0.8 times the tensile strength, are investigated. Additional details about the experimental set up and temperature and shrinkage measurements may be found in /4/.

2.1 Results and Discussion

The loading histories obtained in the tensile creep experiments are shown in Fig. 2. Each test includes two loaded specimens and the variation between the load on each specimen is less than 5%. However, the second specimen at the highest load level, 0.8, failed shortly after application of load and thus only one curve is available at this load level. The reason for the failure is probably dne to damage created during demoulding. The load level is adjusted every 24 hours to the actual fraction of the tensile strength and kept constant for 24 hours. This loading sequence is an attempt to approximate the constant loading procedure for hardened concrete in compression used in /7/. A similar constant tensile loading procedure was used in experiments on hardened concrete in /8/. The concrete was loaded to various constant tensile load levels and the time to failure, the rupture time, was recorded. For relative loadings above 0.6 the concrete were creeping until failnre and both the time before failure

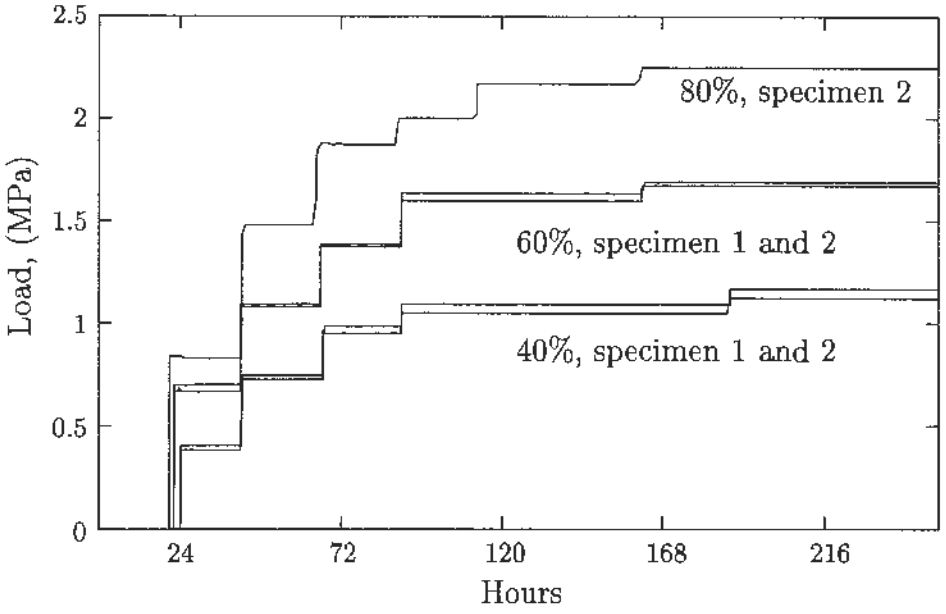

Figure 2: Load history in the tests.

and the ultimate strain decreased significantly with an increase in loading. Below 0.6 there was no failure observed even after 9 months of load.

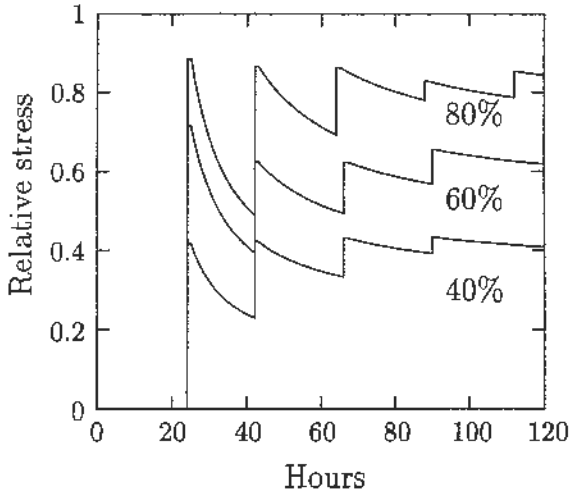

Figure 3: Relative load history in the tests.

The present experiments are stopped after 264 hours and none of the specimens failed within this period. The load level expressed as the fraction of the current tensile strength for the first 120 hours is shown in Fig. 3. The tensile strength development was obtained from one-dimensional dogbone tests, see e.g. /9/. The decrease of the load level is due to the progress of hydration. The load levels aimed at in the tests are mainly fulfilled at the late terms. At the load level of 0.8 the actual values varies from 0.85 to 0.43 within the first 24 hours after loading.

Fig. 4 shows the measured creep compensated for shrinkage and thermal deformations. Each curve in Fig. 4 is the average of the measurements on each side of the specimen. The skewness observed between the two sides was less than 15%. However, the skewness in the second specimen at the 0.6 load level was about 30%, but the average comply with the first specimen. The reason for the skewness may be due to eccentricities or the influence from

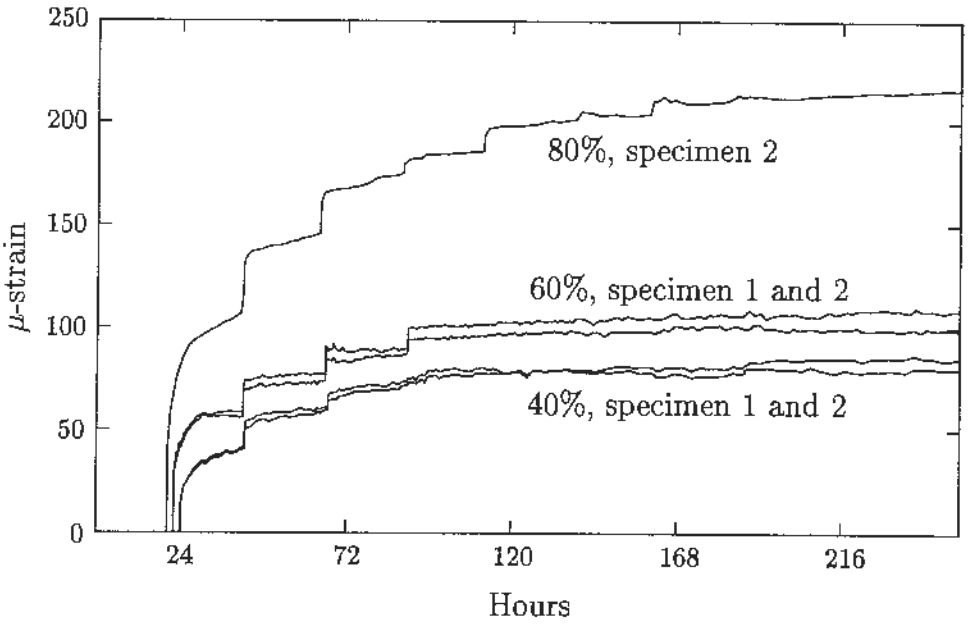

Figure 4: Measured creep in tension.

gravity on the hydration process. For further information see e.g. /4/.
The results in Fig. 4 indicate that non-linearities in creep are absent below the 0.6 load level and significant for the 0.8 load level. The creep responses are integrated results of the loading history and the development of the properties and therefore only a rough estimate of the non-linearities may be given based on Fig. 4. After 250 hours the maximum average value of creep at the three load levels are: 0.4: 82 μ-strain, 0.6: 103 μ-strain and 0.8: 217 μ-strain. This gives the ratios 2.6 and 1.3 between the ultimate creep at the 0.8 and the 0.6 load level and the ultimate creep at the 0.4 load level. Thus the creep at the 0.8 load level is more than two times the creep at 0.4 load level. For the 0.6 load level the observed ratio is less than 1.5 predicted by linearity. The experiments indicate that the non-linear creep starts somewhere in the interval 0.6 to 0.8 times the tensile strength. For a more specific conclusion tensile creep experiments should be carried out where the load is changed continously and kept at a fixed ratio of the tensile strength.
The experimental results in Fig. 4 may be compared with well-known results for non-linearities in compressive creep of hardened concrete. For relative loadings below 0.6 the development of creep seems to be linear, see e.g. /1/, whereas a large non-liuear increase takes place at a higher loading. In concrete structures the compressive load level is normally significantly below 0.6 and therefore the importance of non-linear creep is rather small. However, during the heating period in early age concrete the relative compressive load level may be high due to the low strength values.

3 INCREMENTAL MATERIAL MODELS

In an incremental material model the constitutive law defines a direct relation between stress and strain increments. The hydration process of concrete means that the material is aging, i.e. the material properties develop in time. The response of an aging material is shown in Fig. 5. Initially the state of the material is characterised by the state variables stress, σ, strains, ε, and the modulus of elasticity, $E(t)$. A timestep, Δt, later more cement gel have been formed and this results in an increase of the elastic modulus to $E(t + \Delta t)$. However,

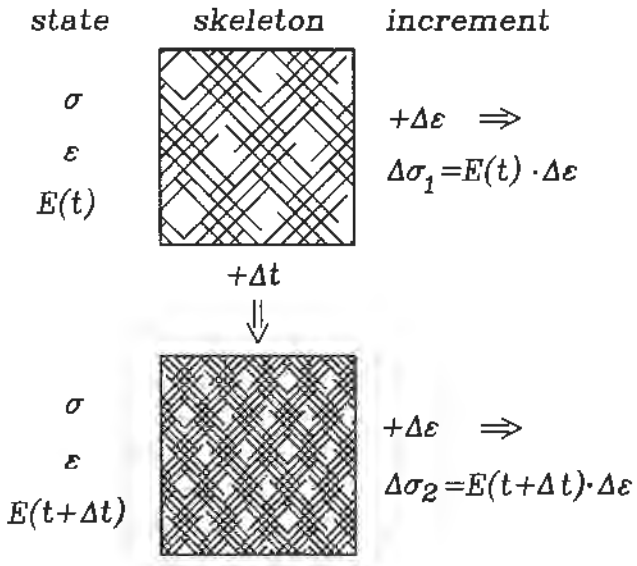

Figure 5: Incremental materials.

the stresses and strains remains unchanged and a strain increment, $\Delta\varepsilon$, at time t only results in the stress increment, $\Delta\sigma_1 = E(t)\,\Delta\varepsilon$, that depends on the actual value of the elastic modulus. The same strain increment at a later stage would result in a larger stress increment, $\Delta\sigma_2 = E(t+\Delta t)\,\Delta\varepsilon$, due to the increased value of the elastic modulus. Thus increments in loading influence for later times and the development of the maturity does not change the stresses per se. The viscoelastic part of the deformation is modelled in the same incremental way, where a damping element gradually develops.
In the incremental model it is easy to include couplings to other factors such as stresses, temperature or water changes. The idea is to define correction factors which are multiplied with the actual material properties. In the present context a stress dependency is included through a stress dependent correction factor multiplied on the properties. In /10/ focus was modelling of thermal effects with temperature dependent factors.

3.1 Incremental Creep Model

The material properties at early age are assumed to depend on the degree of hydration. The starting point is the rheologic model shown in Fig. 6, which consists of an initial spring, a Kelvin cell and a single dashpot. The material properties in the model are the stifnesses $E_0(t)$ and $E_1(t)$ and the viscosities $\eta_1(t)$ and $\eta_2(t)$. Fig. 6 shows that increments of strains and stresses are used to characterise the model. The total strain increment, $\dot{\varepsilon}$, is given by adding the strain increments in each element

$$\dot{\varepsilon} = \dot{\varepsilon}_0 + \dot{\varepsilon}_1 + \dot{\varepsilon}_2 \tag{1}$$

Application of the incremental equilibrium equation gives

$$\ddot{\varepsilon}_1 + \frac{E_1(t) + \dot{\eta}_1(t)}{\eta_1(t)}\,\dot{\varepsilon}_1 = \frac{\dot{\sigma}}{\eta_1(t)} \tag{2}$$

which is the second order differential equation governing a Kelvin cell with time dependent properties. Details about the derivation and solution of (2) may be found in /10/. The idea in the solution procednre is to step forward in timesteps and calculate the stress and

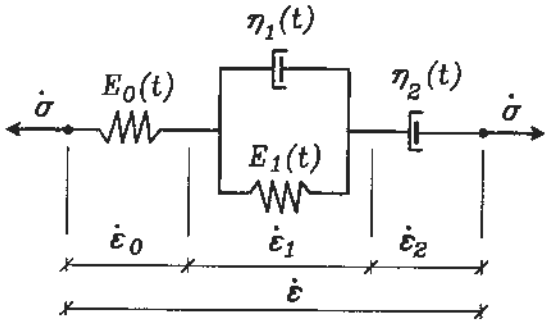

Figure 6: Rheologic model.

strain increments in each timestep. Within a timestep the material properties are considered constants. The model in Fig. 6 may be extended with as many elements as needed but the elements shown have been found to suffice. The final material model may be written

$$\Delta\sigma = \bar{E}_0 \left(\Delta\varepsilon - \Delta\varepsilon_i\right) \tag{3}$$

where $\bar{E}_0$ is the average stiffness within the timestep and ε_i is the sum of the strain increments in the Kelvin cell and the single dashpot. The model is readily suited for implementation in a Finite Element context where ε_i is interpreted as initial strains.
To include the increase in creep at high stress levels the correction factor

$$h(\sigma/f) = 1 - (\sigma/f)^n \tag{4}$$

shown in Fig. 7, has been introduced. The factor, h, is a power function of the relative stress

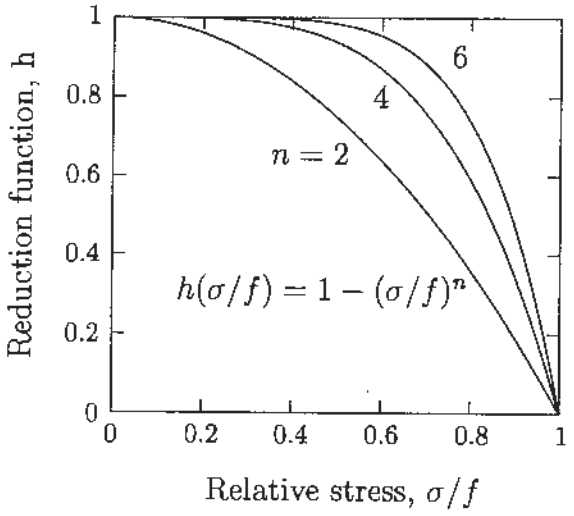

Figure 7: Reductiou function.

level, σ/f, where f is the current strength and σ is the total stress. The influence of the exponent, n, is shown and for higher values the non-linearity occur for higher stress levels. In the case of $n = 6$ non-linearities do not occur at relative stress levels lower than 0.4.
The material properties as functions of the stress level are obtained as

$$E_i(\sigma/f, t) = E_i(t)\, h(\sigma/f) \qquad \eta_i(\sigma/f, t) = \eta_i(t)\, h(\sigma/f) \tag{5}$$

where $E_i(t)$ and $\eta_i(t)$ are the reference development of the actual property at a zero stress level. As shown in (5) all the properties are scaled with the same function. The stress level

could influence the moduli of elasticity different from the viscosities but little is known about this subject. In /10,11/ the couplings to thermal effects are studied. The development of the properties are given by the maturity principle which include the influence from temperature on the progress of hydration. In excess of this the viscosities are scaled with a temperature dependent factor to model the increased mobility of the water in the microstructure with temperature. The influence of temperature on the mobility of the water is defined by the Arrhenius principle and the activation energy for water and this leads to the correction factor. Furthermore, thermodynamic arguments are used to include the concept of microprestresses needed to analyse the magnification of creep due to thermal gradients in time. The microprestresses are large stresses in the microstructure of the cement gel which depend on temperature gradients and drying. Increasing microprestresses increase the creep rate. A combination of several couplings is constructed with one set of factors for each coupling.

3.2 Examples

The analysis of experimental data showed that the reference development of the stiffnesses aud the viscosities in the model could be written in the general form

$$E(t) = ae^{-(b/t)^c} \qquad \text{and} \qquad \eta(t) = a(1 - e^{-t/b})\,(1 - c\,e^{-|(t-f)/d|^e}) \tag{6}$$

where a, b, c, d, e and f are material parameters determined from fitting of data and t is time. The first part of the viscosity, $a(1-e^{-t/b})$, gives an exponential development to the final level a and b gives the rate of growth. The second part, $(1 - c\,e^{-|(t-f)/d|^e})$, is a correction to the exponential development and parameter c gives the magnitude of the correction whereas d and e gives the extension of the correction in time and f gives the location in time of the correction. The development of the strength, f, to be used in (5) is similar to (6). In the analysis of experimental data measured strength values have been fitted to obtain the development in time.

3.2.1 Analysis of the HETEK Tensile Creep Experiments

The experimental data obtained in the HETEK experiments have been analysed with the model and Fig. 8 shows the results.

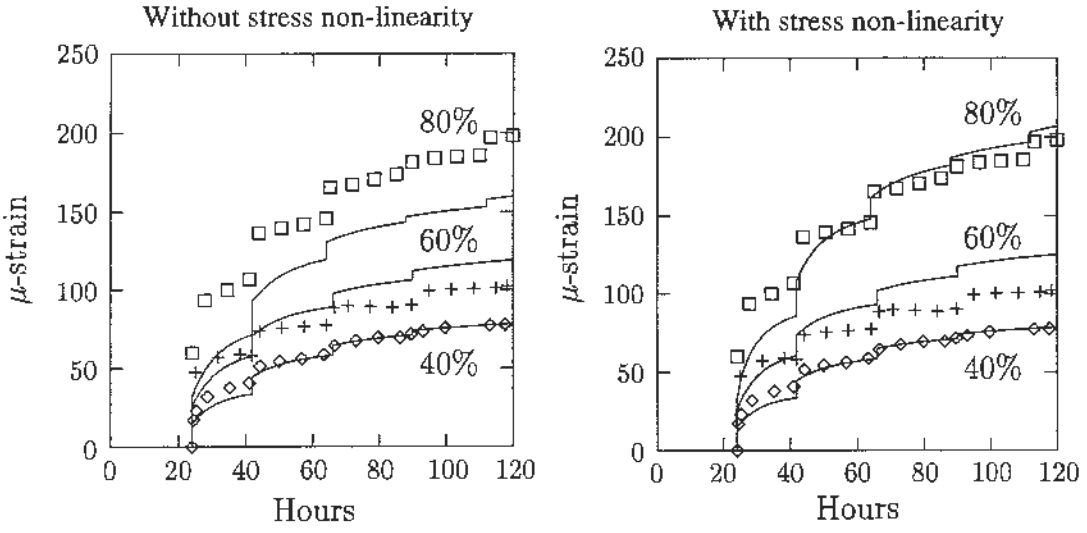

Figure 8: Numerical results, lines, and tensile creep experiments, dots.

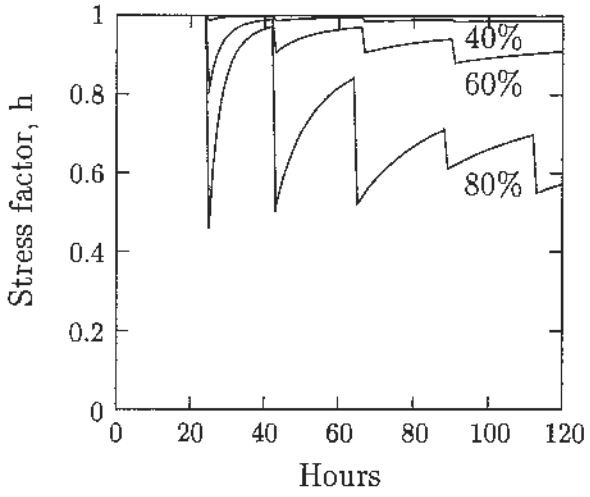

Figure 9: Stress dependent factor used to scale the material properties.

Only the data obtained within the first 120 hours have been used. The later terms have not been analysed because the experiments showed that the creep almost stopped at the two lowest stress levels. This may be due to the problems with the LVDT's. The increase in temperature within the first few hours of the tests has not been included in the analysis. However, it could be included with an extra set of correction functions and the microprestresses.
At each load level the average creep is fitted. The left part shows the results from an analysis without including the stress dependency given in (5) and this corresponds to a linear creep model. At the lowest stress level where little non-linearity occur the agreement is good. The highest load level shows an underprediction of creep of about 25% whereas the intermediate load level shows some overprediction. The right part of Fig. 8 shows the result after introduction of the stress dependent correction factor, (5). The agreement is significantly improved at the highest load level. However, some small discrepancy still remains in the first hours after load application. This may be due to thermal effects which are disregarded.
Fig. 10 shows the resulting development of the four material parameters in the rheologic model after multiplication with the stress dependent factor shown in Fig. 9. The development of the reference moduli of elasticity and viscosities are given by (6) and the parameters in Table 1. For characterisation of the stress non-linearity a value of $n = 5.0$ was determined. The development of the tensile strength used to scale the stresses was given by an exponential development as shown in (6) and $a = 2.9$ MPa, b =26.17 hours and $c = 1.4$.

Table 1: Parameters for the material properties.

	a (GPa)	b (hour)	c	d (hour)	e	f (hour)
E_0	45	10	0.7	-	-	-
E_1	50	35	0.6	-	-	-
η_1/ (hour)	2400	50	0.85	82.0	3.5	-1
η_2/ (hour)	70000	6.7	0.95	89.0	3.55	1

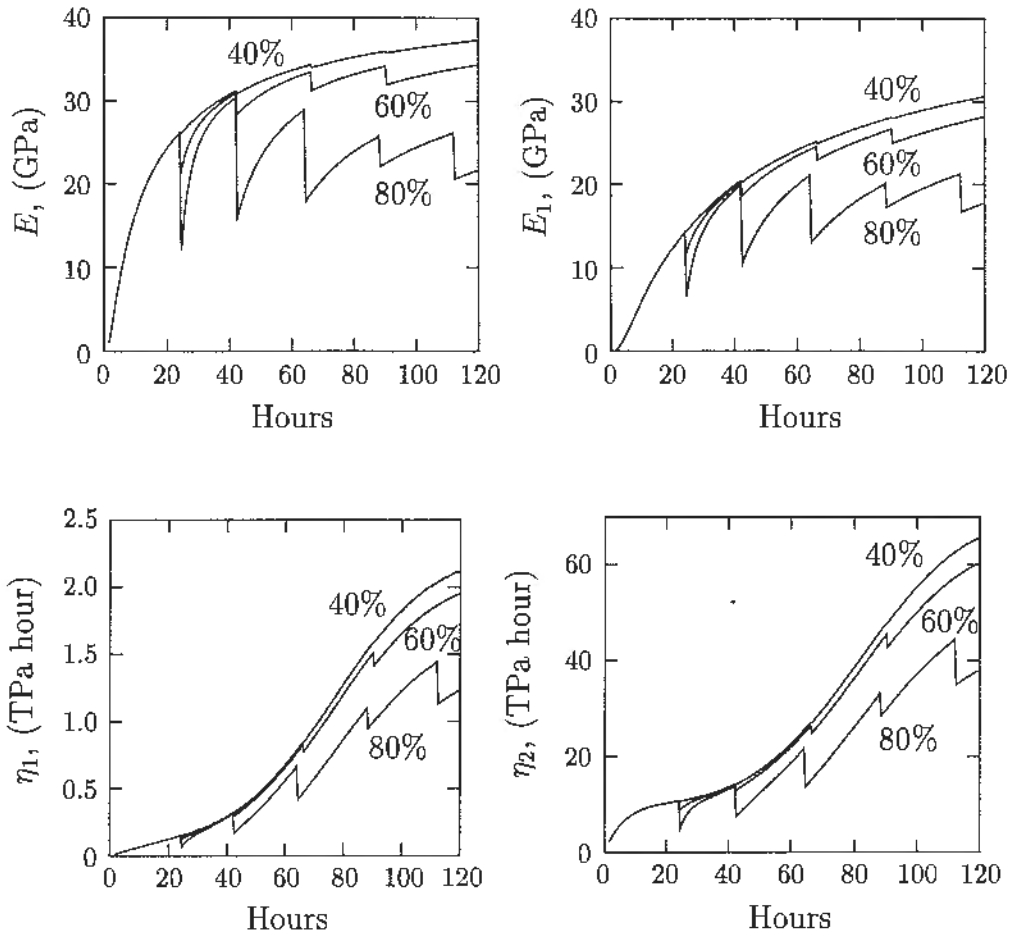

Figure 10: Material properties corrected for stress dependency.

3.2.2 Analysis of Compressive Creep at High Stresses

In /12/ creep of concrete was analysed at different constant compressive load levels.

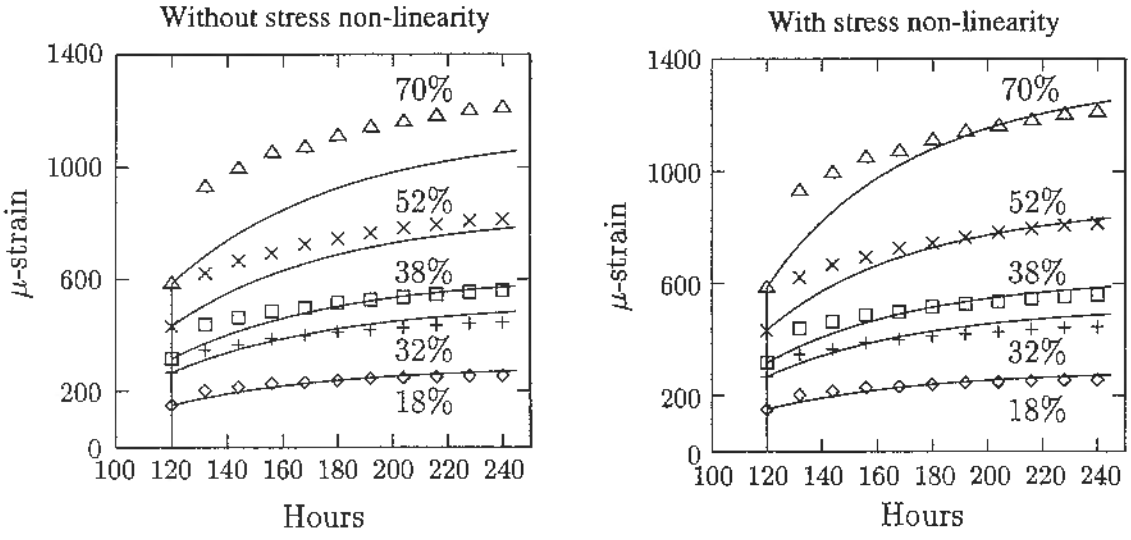

Figure 11: Numerical results, lines, and compressive creep experiments, dots.

The age at loading was 120 hours and the relative load levels were 18%, 32%, 38%, 52% and 70% of the compressive strength at the time at loading. Loading was applied to cylindrical specimens, 300 × 150 mm, and the creep was measured with embedded strain meters. The specimens were sealed with steel membranes and the temperature was kept constant at $20°C$. After 120 hours of hydration the compressive strength was 25 MPa. Fig. 11 shows the results obtained with the model. The left part is obtained without including stress non-linearities and some discrepancy is observed, particularly at the highest load level. The right part shows the mathematical results after introduction of the stress non-linearity and the improvements are significant.

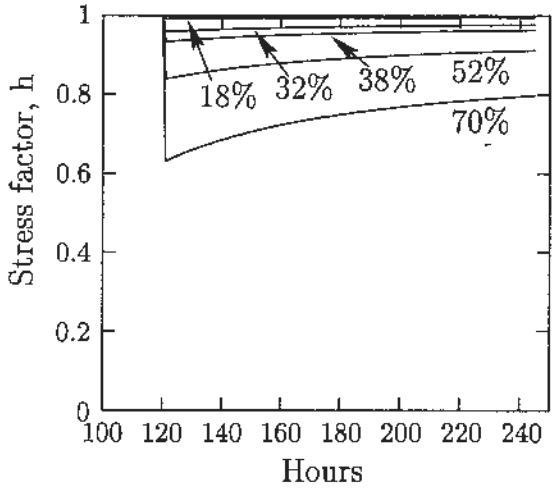

Figure 12: Stress dependent factor used to scale the material properties.

The development of the reference moduli of elasticity and the viscosities are given by (6) and the parameters in Table 2.

Table 2: Parameters for the material properties.

	a (GPa)	b (hour)	c	d (hour)	e	f (hour)
E_0	36	10	0.7	-	-	-
E_1	50	35	0.6	-	-	-
η_1/ (hour)	2300	66.7	0.88	82.0	3.5	-1
η_2/ (hour)	120000	5.0	0.95	94.9	3.5	25

Fig. 12 shows the correction factor used to scale the material properties. The stress factor only increase 0.17 even at the highest stress level and this is due to the high age at loading where most of the hydration has taken place. The exponent was determined to $n = 2.8$ and the development of the compressive strength was given by (6) and $a = 39.4$ MPa, $b = 50$ honrs and $c = 0.9$. Fig. 13 shows the resulting development of the material properties.

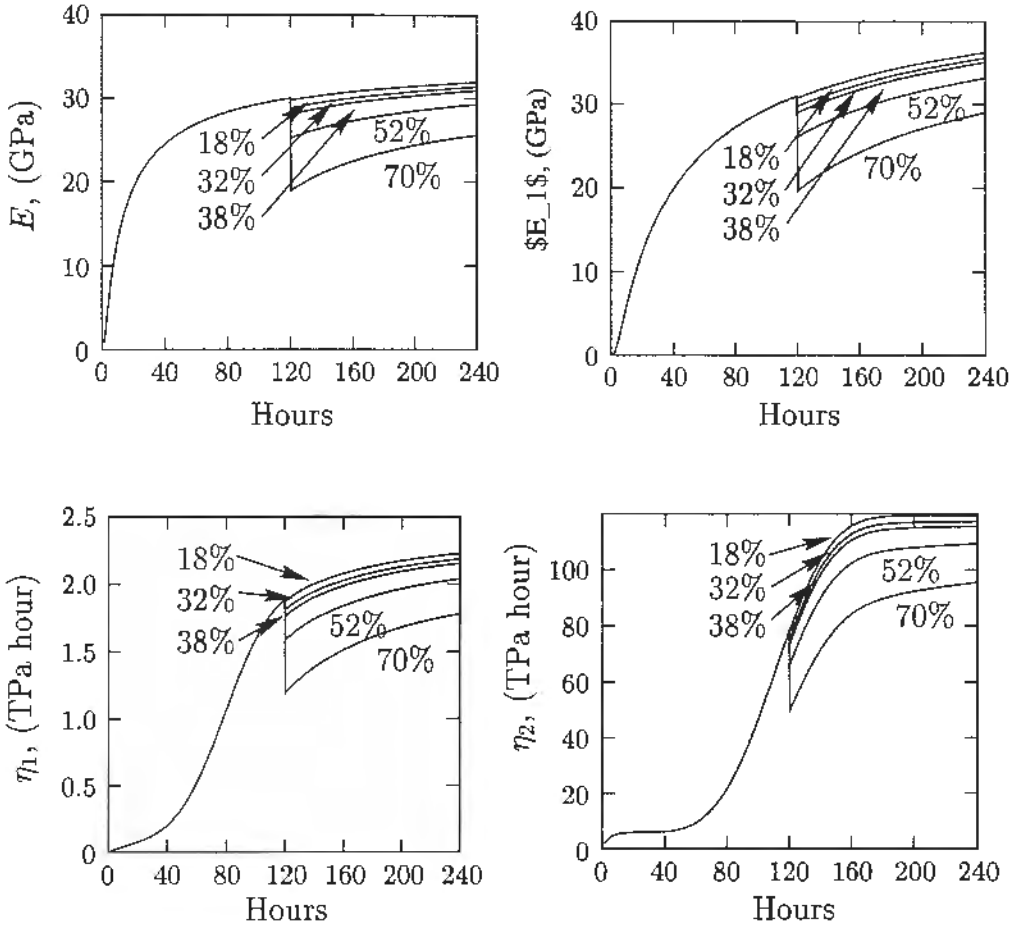

Figure 13: Material properties corrected for stress dependency.

4 CONCLUSION

A mathematical model for the analysis of non-linear creep is set up. The model consists of a spring, a Kelvin cell and a single dashpot coupled in series. The formulation is incremental and hereby the model is related to the incremental process of hydration where new layers of cement gel are build up in a stress free state. The increase of creep at high stress levels is included in the model by multiplying the material properties with a stress dependent factor. For higher stress levels the factor decreases and a simple power function is used with only one parameter.

Tensile creep experiments at high relative stresses have been carried out in the HETEK project. The age at first loading was 24 hours. The specimens were dogbone shaped and the test procedure has been described. The results indicate that non-linearities in tensile creep start in the range from 60% to 80% of the tensile strength. The model has been used for the analysis of the results and it is found that the stress correction significantly improves the results. Furthermore, compressive creep results, where the load levels are in the range 18% to 70% of the compressive strength, have been analysed. The improvements cansed by the stress correction are significant also in this case.

4.1 Acknowledgement

The support from The Danish Technical Research Council, Grant No. 9601503 is greatly appreciated.

5 REFERENCES

/1/ A. M. Neville, W. H. Dilger, and J. J. Brooks. *Creep of Plain and Structural Concrete.* Construction Press, 1983.

/2/ F. H. Wittmann. "Bestimmung physikalischer Eigenschaften des Zementsteins". In *Deutscher Ausschuss für Stahlbeton*, 232, pages 1–63. Vertrieb Durch Verlag von Wilhelm Ernst & Sohn, 1980.

/3/ K. van Breugel. "Relaxation of Young Concrete". Technical report, Technische Hogeschool Delft, Afdeling der Civiele Techniek, 1980.

/4/ A. B. Hauggaard, L. Damkilde, P. Freiesleben Hansen, J. Hougaard Hansen, A. Nielsen, and S. L. Christensen. "HETEK, Control of Early Age Cracking in Concrete, Phase 3: Creep in Concrete". Series I 13, Department of Structural Engineering and Materials, Technical University of Denmark, 1997.

/5/ Danish Standard, DS 423.24. Testing of concrete – Hardened concrete, Tensile strength, DS 423.24. The Steering Committee of DIF's Codes of Practice Organization, Teknisk Forlag, Skelbækgade 4, DK-1717 Copenhagen V, 1984.

/6/ J. Byfors. *Plain Concrete at Early Ages.* CBI Research, Swedish Council for Building Research, 1980.

/7/ H. Rñsch. "Researches toward a general flexural theory for structural concrete". *Proceedings for the American Concrete Institute*, 57(1):1–28, 1960.

/8/ M. A. Al-Kubaisy and A. G. Young. "Failure of concrete under sustained tension". *Magazine of Concrete Research*, 27(92):171–178, 1975.

/9/ A. B. Hauggaard, L. Damkilde, and P. Freiesleben Hansen. "Tensile Strength of Concrete at Early Ages - Experimental and Numerical Analysis". *Submitted for publication in Cement and Concrete Research*, 1997.

/10/ A. B. Hauggaard, L. Damkilde, and P. Freiesleben Hansen. "Transitional Thermal Creep of Early Age Concrete". *Submitted for publication in Journal of Engineering Mechanics*, 1997.

/11/ A. B. Hauggaard. *Mathematical Modelling and Experimental Analysis of Early Age Concrete.* PhD thesis, Department of Structural Engineering and Materials, Technical University of Denmark, 1997.

/12/ K. Iriya, M. Hiramoto, T. Hattori, and H. Umehara. "Creep Behaviour for Early Aged Concrete". Technical report, Nagoya Institute of Technology, Department of Civil Engineering, Gokiso-Cho Showa-Ku, Nagoya, Japan, 1997.